

International Conference on  
**PROBABILISTICS IN GEOTECHNICS**  
Technical and Economic Risk Estimation

Edited by  
Rudolf Pöttler, Herbert Klapperich, Helmut F. Schweiger



15 - 19 September 2002 · Graz, Austria

---

**VGE**  
Verlag Glückauf Essen

## **Probabilistic Geotechnical Analysis: How difficult does it need to be?**

D. V. Griffiths, Professor  
Geomechanics Research Center, Colorado School of Mines  
Golden, CO 80401, U.S.A.  
Tel: 303 273 3669; Email: d.v.griffiths@mines.edu

Gordon A. Fenton, Professor  
Department of Engineering Mathematics, Dalhousie University  
Halifax, NS B3J 2X4, CANADA  
gordon.fenton@dal.ca

Derena E. Tveten, Research Assistant  
Geomechanics Research Center, Colorado School of Mines  
Golden, CO 80401, U.S.A.  
dtveten@mines.edu

### **Abstract**

The paper reviews some established probabilistic analysis techniques, such as the “First Order Second Moment” and the “Point Estimate” methods, as applied to geotechnical problems. The advantages and limitations of these methods are discussed, with particular reference to the role of spatial correlation which typically is not accounted for in these simple methods. The paper goes on to describe a more rigorous approach to probabilistic geotechnical analysis, in which random field and finite element methodologies are merged. The results highlight cases in which proper modeling of spatial correlation is important, and illustrates this through a simple example relating to triaxial compression of a frictional soil.

## **1 Introduction**

Many sources of uncertainty exist in geotechnical analysis ranging from the material parameters to the sampling and testing techniques. This paper addresses the question of how variable material parameters impact the safety and, ultimately, the economics of geotechnical design.

Traditional geotechnical analysis uses the “Factor of Safety” approach in one of two ways. In foundations analysis for example, Terzaghi’s bearing capacity equation leads to an estimate of the ultimate value, which is then divided by the Factor of Safety to give allowable loading levels for design. Alternatively, in slope stability analysis, the Factor of

Safety is included by reducing the shear strength of the soil prior to performing a limit equilibrium calculation. Either way, the Factor of Safety represents a blanket factor that implicitly includes all sources of variability and uncertainty inherent in the geotechnical analysis.

The approaches described in this paper attempt to include the effects of soil property variability in a more scientific way using statistical methods. If it is assumed that the soil parameters in question (e.g. friction angle, cohesion, compressibility and permeability) are random variables that can be expressed in the form of a probability density function, then the issue becomes one of estimating the probability density function of some outcome that depends on the input random variables. The output can then be interpreted in terms of probabilities, leading to statements such as: “The design load on the foundation will give a probability of bearing capacity failure of  $p_1\%$ ”, “The embankment has a probability of slope failure of  $p_2\%$ ”, “The probability of the design settlement levels being exceeded is  $p_3\%$ ”, or “The probability of the seepage level exceeding the design limit is  $p_4\%$ ”.

A thorough understanding of how random variables affect the functions that depend on them is essential. The first part of the paper therefore summarises some of the fundamental rules that describe this relationship.

## 2 Some rules describing random variables

In this section, the notation is quite generic with random variables (e.g.  $X$  and  $Y$ ) denoted in upper case. Later in the paper, specific geotechnical examples will be included.

### Expectation

Let a random variable  $X$  be described by the Probability Density Function (PDF),  $f_X(x)$ .

If  $g(X)$  is a function of the random variable  $X$ , then the expected value of  $g(X)$ , is its average value after it has been weighted by the Probability Density Function:

$$E[g(X)] = \int_{-\infty}^{\infty} g(x)f_X(x) dx \quad (1)$$

### Moments

First Moment: Mean

$$\mu_x = E[X] = \int_{-\infty}^{\infty} xf_X(x) dx \quad (2)$$

Second Moment: Variance

$$V[X] = \sigma_x^2 = E[(X - \mu_x)^2] = \int_{-\infty}^{\infty} (x - \mu_x)^2 f_X(x) dx \quad (3)$$

Third Moment: Skewness

$$\nu_x = \frac{E[(X - \mu_x)^3]}{\sigma_x^3} = \frac{1}{\sigma_x^3} \int_{-\infty}^{\infty} (x - \mu_x)^3 f_X(x) dx \quad (4)$$

### Identities relating to Expectation

A linear function of two random variables  $X$  and  $Y$

$$E[a + bX + cY] = a + bE[X] + cE[Y] \quad (5)$$

The sum of multiple random variables  $X_1, X_2, \dots$  etc.

$$E[X_1 + X_2 + \dots + X_n] = E[X_1] + E[X_2] + \dots + E[X_n] \quad (6)$$

The sum of functions of two random variables,  $X$  and  $Y$

$$E[f(X) + g(Y)] = E[f(X)] + E[g(Y)] \quad (7)$$

A nonlinear function of two random variables  $X$  and  $Y$  can be expressed using a Taylor series expansion

$$\begin{aligned} f(X, Y) = & f(E[X], E[Y]) + (X - E[X])\frac{\partial f}{\partial x} + (Y - E[Y])\frac{\partial f}{\partial y} \\ & + \frac{1}{2}(X - E[X])^2\frac{\partial^2 f}{\partial x^2} + \frac{1}{2}(Y - E[Y])^2\frac{\partial^2 f}{\partial y^2} \\ & + \frac{1}{2}(X - E[X])(Y - E[Y])\frac{\partial^2 f}{\partial x \partial y} \\ & + \frac{1}{2}(Y - E[Y])(X - E[X])\frac{\partial^2 f}{\partial y \partial x} + \dots \end{aligned} \quad (8)$$

where all derivatives are evaluated at the mean. Thus to a first order of accuracy:

$$E[f(X, Y)] = f(E[X], E[Y]) \quad (9)$$

and to a second order:

$$\begin{aligned} E[f(X, Y)] = & f(E[X], E[Y]) + \frac{1}{2}V[X]\frac{\partial^2 f}{\partial x^2} + \frac{1}{2}V[Y]\frac{\partial^2 f}{\partial y^2} \\ & + \text{cov}[X, Y]\frac{\partial^2 f}{\partial x \partial y} \end{aligned} \quad (10)$$

### **Identities relating to Variance**

Variance of a random variable  $X$

$$\begin{aligned} V[X] &= E[(X - \mu_x)^2] \\ &= E[X^2] - (E[X])^2 \end{aligned} \quad (11)$$

Variance of a linear function of  $X$

$$\begin{aligned} V[a + bX] &= b^2 E[(X - \mu_x)^2] \\ &= b^2 V[X] \end{aligned} \quad (12)$$

Variance of a linear function of two random variables  $X$  and  $Y$

$$V[a + bX + cY] = b^2 V[X] + c^2 V[Y] + 2bc \text{cov}[X, Y] \quad (13)$$

Variance of a linear function of uncorrelated random variables

$$V[a_0 + a_1 X_1 + a_2 X_2 + \dots + a_n X_n] = a_1^2 V[X_1] + a_2^2 V[X_2] + \dots + a_n^2 V[X_n] \quad (14)$$

## Covariance and Correlation

Covariance

$$\begin{aligned}\text{cov}[X, Y] &= E[(X - \mu_x)(Y - \mu_y)] \\ &= E[XY] - E[X]E[Y]\end{aligned}\quad (15)$$

$$\begin{aligned}\text{cov}[X, X] &= E[(X - \mu_x)^2] \\ &= E[X^2] - (E[X])^2 \\ &= V[X] \\ &= \sigma_x^2\end{aligned}\quad (16)$$

Correlation Coefficient

$$\begin{aligned}\rho &= \frac{\text{cov}[X, Y]}{\sigma_x \sigma_y} \\ -1 &\leq \rho \leq 1\end{aligned}\quad (17)$$

## 3 The First Order Second Moment (FOSM) Method

The First Order Second Moment (FOSM) method is a relatively simple method of including the effects of variability of input variables on a resulting dependent variable

The First Order Second Moment method uses a Taylor series expansion of the function to be evaluated. This expansion is truncated after the linear term, (hence “first order”). The modified expansion is then used, along with the first two moments of the random variable(s), to determine the values of the first two moments of the dependent variable (hence “second moment”).

Due to truncation of the Taylor series after first order terms, the accuracy of the method deteriorates if second and higher derivatives of the function are significant. Furthermore, the method takes no account of the form of the probability density function, describing the random variables using only their mean and standard deviation. The skewness (third moment) is ignored.

Another limitation of the traditional FOSM method is that explicit account of spatial correlation of the random variable is not typically done. For example, the soil properties at two geotechnical sites could have identical mean and standard deviations, however at one site, the properties could vary rapidly from point to point (“low” spatial correlation length), and at another they could vary gradually (“high spatial correlation length”). This issue will be returned to later in the paper.

Consider a function  $f(X, Y)$  of two random variables  $X$  and  $Y$ . The Taylor Series expansion of the function about the mean values  $(\mu_x, \mu_y)$ , truncated after first order terms from equation (8), gives:

$$f(X, Y) = f(\mu_x, \mu_y) + (X - \mu_x) \frac{\partial f}{\partial x} + (Y - \mu_y) \frac{\partial f}{\partial y}\quad (18)$$

where derivatives are evaluated at  $(\mu_x, \mu_y)$ .

To a first order of accuracy, the expected value of the function is given by equation (9), and the variance by,

$$V[f(X, Y)] = V\left[(X - \mu_x) \frac{\partial f}{\partial x} + (Y - \mu_y) \frac{\partial f}{\partial y}\right]\quad (19)$$

hence,

$$V[f(X, Y)] = \left(\frac{\partial f}{\partial x}\right)^2 V[X] + \left(\frac{\partial f}{\partial y}\right)^2 V[Y] + 2\frac{\partial f}{\partial x}\frac{\partial f}{\partial y}\text{cov}[X, Y] \quad (20)$$

If  $X$  and  $Y$  are uncorrelated,

$$V[f(X, Y)] = \left(\frac{\partial f}{\partial x}\right)^2 V[X] + \left(\frac{\partial f}{\partial y}\right)^2 V[Y] \quad (21)$$

In general, for a function of  $n$  uncorrelated random variables, the FOSM Method gives:

$$V[f(X_1, X_2, \dots, X_n)] = \sum_{i=1}^n \left(\frac{\partial f}{\partial x_i}\right)^2 V[X_i] \quad (22)$$

where the first derivatives are evaluated at the mean values  $(\mu_{x_1}, \mu_{x_2}, \dots, \mu_{x_n})$

### FOSM Example: Unconfined triaxial compression of a $c'$ , $\phi'$ soil

The unconfined ( $\sigma'_3 = 0$ ) compressive strength of a drained  $c'$ ,  $\phi'$  soil is given from the Mohr-Coulomb equation as:

$$q_u = 2c' \tan(45 + \phi'/2) \quad (23)$$

Considering the classical Coulomb shear strength law:

$$\tau_f = \sigma' \tan \phi' + c' \quad (24)$$

it is more fundamental to deal with  $\tan \phi'$  (rather than  $\phi'$ ) as the random variable. Thus equation (23) has been rearranged as:

$$q_u = 2c' [\tan \phi' + (1 + \tan^2 \phi')^{1/2}] \quad (25)$$

Treating  $c'$  and  $\tan \phi'$  as uncorrelated random variables,

$$\mu_{q_u} = 2\mu_{c'} [\mu_{\tan \phi'} + (1 + \mu_{\tan \phi'}^2)^{1/2}] \quad (26)$$

and referring to equation (22),

$$\sigma_{q_u}^2 = V[q_u] = \left(\frac{\partial q_u}{\partial c'}\right)^2 V[c'] + \left(\frac{\partial q_u}{\partial(\tan \phi')}\right)^2 V[\tan \phi'] \quad (27)$$

The required derivatives computed analytically are given by:

$$\frac{\partial q_u}{\partial c'} = 2[\tan \phi' + (1 + \tan^2 \phi')^{1/2}] \quad (28)$$

and

$$\frac{\partial q_u}{\partial(\tan \phi')} = 2c' \left[1 + \frac{\tan \phi'}{(1 + \tan^2 \phi')^{1/2}}\right] \quad (29)$$

It is now possible to compute the mean and standard deviation of the unconfined compressive strength for a range of soil property variances.

As an example, let  $\mu_{c'} = 100$  kPa and  $\mu_{\tan \phi'} = \tan 30^\circ = 0.577$ . To a first order of approximation, the mean value of the unconfined compressive strength is given by

$\mu_{q_u} = 346.4$  kPa. Consider now a range of standard deviation values on these input variables expressed in the dimensionless form of a Coefficient of Variation (*C.O.V.*). In this example, the *C.O.V.* values for both  $c'$  and  $\tan \phi'$  are the same, thus

$$C.O.V._{c', \tan \phi'} = \frac{\sigma_{c'}}{\mu_{c'}} = \frac{\sigma_{\tan \phi'}}{\mu_{\tan \phi'}} \quad (30)$$

The partial derivatives of the unconfined compressive strength evaluated at the mean, from equations (28) and (29) are given by  $\partial q_u / \partial c' = 3.46$  and  $\partial q_u / \partial (\tan \phi') = 300$  kPa. Hence for a range of input *C.O.V.* $_{c', \tan \phi'}$  values, Table 1 gives the predicted mean and standard deviation of the unconfined compressive strength from equations (26) and (27).

**Table 1. Statistics of  $q_u$  predicted using FOSM (analytical approach)**

<i>C.O.V.</i> $_{c', \tan \phi'}$	$V[c']$ (kPa) <sup>2</sup>	$V[\tan \phi']$	$V[q_u]$ (kPa) <sup>2</sup>	$\sigma_{q_u}$ (kPa)	$\mu_{q_u}$ (kPa)	<i>C.O.V.</i> $_{q_u}$
0.1	100	0.0033	1500.0	38.7	346.4	0.11
0.3	900	0.0300	13500.0	116.2	346.4	0.34
0.5	2500	0.0833	37500.0	193.6	346.4	0.56
0.7	4900	0.1633	73500.0	271.1	346.4	0.78
0.9	8100	0.2700	121500.0	348.6	346.4	1.01

### Numerical approach

An alternative approach evaluates the derivatives numerically, using a central finite difference formula. In this case, the dependent variable,  $q_u$ , is sampled across two standard deviations in one variable, while keeping the other variable fixed at the mean. This large central difference interval encompasses about 68% of all values of the input parameters  $c'$  and  $\tan \phi'$ , so the approximation is only reasonable if the function  $q_u(c', \tan \phi')$  from equation (25), does not exhibit much nonlinearity across this range. The finite difference formulas take the form:

$$\frac{\partial q_u}{\partial c'} \approx \frac{q_u(\mu_{c'} + \sigma_{c'}, \mu_{\tan \phi'}) - q_u(\mu_{c'} - \sigma_{c'}, \mu_{\tan \phi'})}{2\sigma_{c'}} = \frac{\Delta q_u(c')}{2\sigma_{c'}} \quad (31)$$

and

$$\frac{\partial q_u}{\partial (\tan \phi')} \approx \frac{q_u(\mu_{c'}, \mu_{\tan \phi'} + \sigma_{\tan \phi'}) - q_u(\mu_{c'}, \mu_{\tan \phi'} - \sigma_{\tan \phi'})}{2\sigma_{\tan \phi'}} = \frac{\Delta q_u(\tan \phi')}{2\sigma_{\tan \phi'}} \quad (32)$$

The main attraction of this approach, is that once the derivative terms are squared and substituted into equation (27), the variances of  $c'$  and  $\tan \phi'$  cancel out, leaving:

$$V[q_u] \approx \left( \frac{\Delta q_u(c')}{2} \right)^2 + \left( \frac{\Delta q_u(\tan \phi')}{2} \right)^2 \quad (33)$$

In this case,  $q_u$  is a linear function of  $c'$  and is slightly nonlinear with respect to  $\tan \phi'$ . It is clear from a comparison of Tables 1 and 2, that the numerical and analytical approaches in this case give essentially the same results.

**Table 2. Statistics of  $q_u$  predicted using FOSM (numerical approach)**

$C.O.V._{c', \tan \phi'}$	$\frac{\Delta q_u(c')}{2}$	$\frac{\Delta q_u(\tan \phi')}{2}$	$V[q_u]$	$\sigma_{q_u}$	$\mu_{q_u}$	$C.O.V._{q_u}$
	(kPa)	(kPa)	(kPa) <sup>2</sup>	(kPa)	(kPa)	
0.1	34.64	17.31	1499.8	38.7	346.4	0.11
0.3	103.93	51.82	13484.9	116.1	346.4	0.34
0.5	173.21	85.94	37385.6	193.4	346.4	0.56
0.7	242.49	119.46	73070.5	270.3	346.4	0.78
0.9	311.77	152.19	120362.7	346.9	346.4	1.00

**Refined approach including second order terms**

In the above example, a first order approximation was used to predict both the mean and variance of  $q_u$  from equations (9) and (19). Since the variances of  $c'$  and  $\tan \phi'$  are both known, it is possible to refine the estimate of  $\mu_{q_u}$  by including second order terms from equation (10) leading to:

$$\begin{aligned} \mu_{q_u} = & q_u(\mu_{c'}, \mu_{\tan \phi'}) + \frac{1}{2}V[c'] \frac{\partial^2 q_u}{\partial c'^2} + \frac{1}{2}V[\tan \phi'] \frac{\partial^2 q_u}{\partial (\tan \phi')^2} \\ & + \text{cov}[c', \tan \phi'] \frac{\partial^2 q_u}{\partial c' \partial (\tan \phi')} \end{aligned} \quad (34)$$

where all derivatives are evaluated at the mean. Noting that in this case  $\partial^2 q_u / \partial c'^2 = 0$ , and  $\text{cov}[c', \tan \phi'] = 0$ , the expression simplifies to:

$$\mu_{q_u} = q_u(\mu_{c'}, \mu_{\tan \phi'}) + \frac{1}{2}V[\tan \phi'] \frac{\partial^2 q_u}{\partial (\tan \phi')^2} \quad (35)$$

so the analytical form of the second derivative is given by:

$$\frac{\partial^2 q_u}{\partial (\tan \phi')^2} = 2c' \left( \frac{1}{(1 + \tan^2 \phi')^{1/2}} - \frac{\tan^2 \phi'}{(1 + \tan^2 \phi')^{3/2}} \right) \quad (36)$$

Combining equations (35) and (36) for the particular case of  $\mu_{c'} = 100$  kPa and  $\mu_{\tan \phi'} = 0.577$  leads to:

$$\mu_{q_u} = 346.41 + 64.95 V[\tan \phi'] \text{ kPa} \quad (37)$$

Table 3 shows a reworking of the analytical results from Table 1 including second order terms in the estimation of  $\mu_{q_u}$ . A comparison of the results from the two tables indicates that the second order terms have marginally increased  $\mu_{q_u}$  and thus reduced  $C.O.V._{q_u}$ , but the differences are barely noticeable until the input variance becomes relatively large.

**Table 3. Statistics of  $q_u$  predicted using FOSM (analytical approach including second order terms)**

$C.O.V._{c', \tan \phi'}$	$V[\tan \phi']$	$\sigma_{q_u}$	$\mu_{q_u}$	$C.O.V._{q_u}$
		(kPa)	(kPa)	
0.1	0.0033	38.7	346.6	0.11
0.3	0.0300	116.2	348.4	0.33
0.5	0.0833	193.6	351.8	0.55
0.7	0.1633	271.1	357.0	0.76
0.9	0.2700	348.6	363.9	0.96



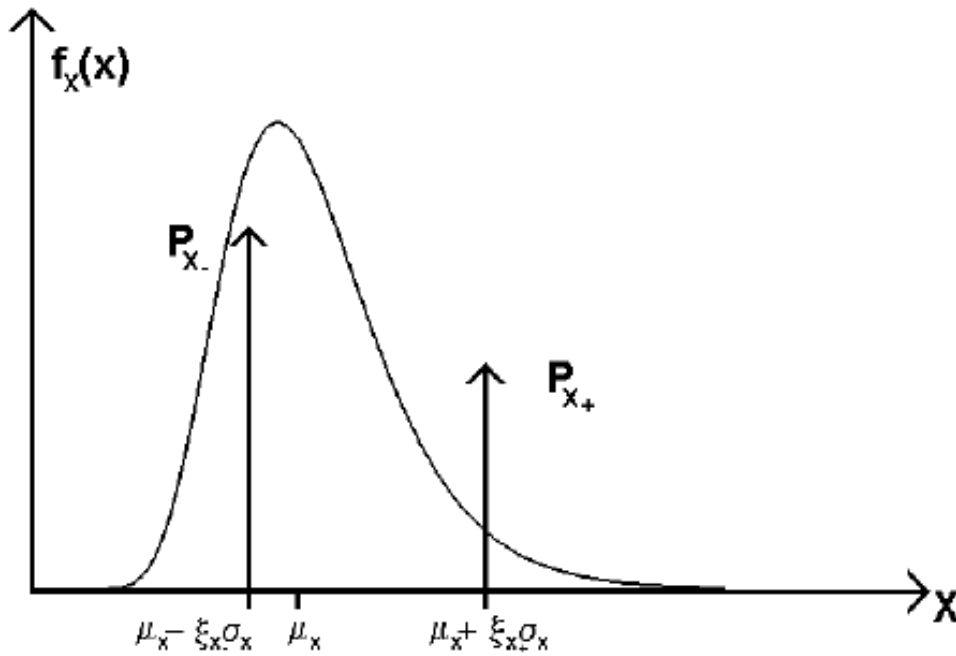


Figure 1: PEM Distribution

## 4 The Point Estimate Method (PEM)

The Point Estimate Method (PEM) is an alternative way of taking into account random variables. Like FOSM, PEM does not require knowledge of the particular form of the probability density function of the input, however PEM is able to account for up to three moments (mean  $\mu$ , variance  $\sigma^2$ , and skewness  $\nu$ ). As with FOSM, PEM does not typically explicit account for spatial correlation.

PEM is essentially a weighted average method reminiscent of numerical integration formulas involving “sampling points” and “weighting parameters”. The point estimate method reviewed here will be the two point estimate method developed by Rosenblueth (1975, 1981) and also described by Harr (1987).

The Point Estimate Method seeks to replace a continuous probability density function, with a discrete function having the same first three central moments.

### Steps for implementing PEM

1. Determine the relationship between the dependent variable and random input variables  $W = f(X, Y, \dots)$
2. Compute the locations of the two sampling points for each input variable. For a single random variable  $X$ , with skewness  $\nu_x$ , the sampling points are given by:

$$\xi_{x+} = \frac{\nu_x}{2} + \left(1 + \left(\frac{\nu_x}{2}\right)^2\right)^{1/2} \quad (38)$$

and

$$\xi_{x-} = \xi_{x+} - \nu_x \quad (39)$$

where  $\xi_{x+}$  and  $\xi_{x-}$  are standard deviation units giving the locations of the sampling points to the right and left of the mean respectively. Figure 1 shows these sampling points located at  $\mu_x + \xi_{x+}\sigma_x$  and  $\mu_x - \xi_{x-}\sigma_x$

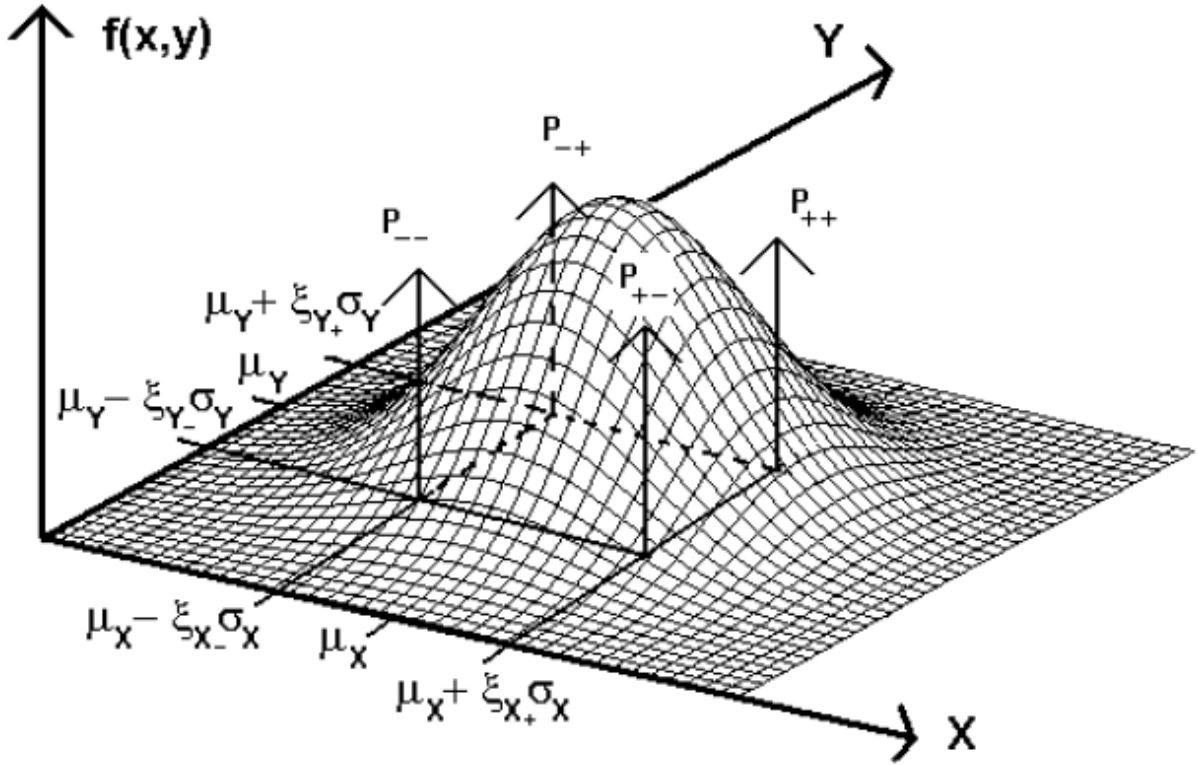


Figure 2: Point Estimates for two random variables

If the function depends on  $n$  variables, there will be  $2^n$  sampling points corresponding to all combinations of the two sampling points for each variable. Figure 2 shows the locations of sampling points for a distribution of two random variables  $X$  and  $Y$ . Since  $n = 2$  there are four sampling points given by

$$\begin{aligned}
 &(\mu_X + \xi_{X+} \sigma_X, \mu_Y + \xi_{Y+} \sigma_Y) \\
 &(\mu_X + \xi_{X+} \sigma_X, \mu_Y - \xi_{Y-} \sigma_Y) \\
 &(\mu_X - \xi_{X-} \sigma_X, \mu_Y + \xi_{Y+} \sigma_Y) \\
 &(\mu_X - \xi_{X-} \sigma_X, \mu_Y - \xi_{Y-} \sigma_Y)
 \end{aligned}$$

If skewness is ignored or assumed to equal zero, from equations (38) and (39),

$$\xi_{X+} = \xi_{X-} = \xi_{Y+} = \xi_{Y-} = 1 \quad (40)$$

and each random variable has point locations that are plus and minus one standard deviation from the mean.

3. Determine the weights  $P_i$ , to give each of the  $2^n$  point estimates. Just as a probability density function encloses an “area” of unity, so the probability weights must also sum to unity. The weights can also take into account correlation between two or more random variables.

For a single random variable  $X$ , the weights are given by:

$$P_{X+} = \xi_{X-} / (\xi_{X+} + \xi_{X-}) \quad (41)$$

$$P_{x_-} = 1 - P_{x_+} \quad (42)$$

For  $n$  random variables with no skewness, Christian et al (1999) have presented a general expression for finding the weights, which takes into account the correlation coefficient  $\rho_{ij}$  between the  $i^{th}$  and  $j^{th}$  variables as follows:

$$P_{s_1 s_2 \dots s_n} = 1/2^n (1 + \sum_{i=1}^{n-1} \sum_{j=i+1}^n (s_i s_j \rho_{ij})) \quad (43)$$

$s_i$  takes the sign + for points greater than the mean, and – for points smaller than the mean. The sign product  $s_i s_j$  under the summation, determines the sign of the correlation coefficient, and the subscripts of the weight  $P$  indicate the location of the point that is being weighted. For example, for a point evaluated at  $(x_1, y_1) = (\mu_x + \sigma_x, \mu_y - \sigma_y)$ ,  $s_1 = +$  and  $s_2 = -$  resulting in a negative product with a weight denoted by  $P_{+-}$ .

For multiple random variables where skewness cannot be disregarded, the computation of weights is significantly more complicated. Rosenblueth(1981) presents the weights for the case of  $n=2$  to be the following:

$$P_{s_1 s_2} = P_{X_{s_1}} * P_{Y_{s_2}} + s_1 s_2 * [\rho_{XY} / ((1 + (\nu_x/2)^3)(1 + (\nu_y/2)^3)^{1/2})] \quad (44)$$

The notation is the same as for the previous equation with  $P_{X_{s_i}}$  and  $P_{Y_{s_j}}$  being the weights for variables X and Y evaluated as a single random variables(see eqns (41) and (42)).  $\nu_{X/Y}$  is the skewness of the random variable distribution. For a lognormal distribution, the skewness coefficient,  $\nu$ , can be calculated from the *C.O.V.* as follows (e.g. Benjamin and Cornell 1970):

$$\nu = 3 * C.O.V. + C.O.V.^3 \quad (45)$$

4. Determine the value of the dependent variable at each point. Let these values be denoted by  $W_{X(+ \text{ or } -), Y(+ \text{ or } -), \dots}$ , depending upon the point at which  $W$  is being evaluated. For  $n$  random input variables,  $W$  is evaluated at  $2^n$  points.
5. In general, the Point Estimate Method enables us to estimate the expected values of the first three moments of the dependent variable using the following summations. Here, the  $P_i$  and  $W_i$  are the weight and the value of the dependent variable associated with some point location  $i$  where  $i$  ranges from 2 to  $2^n$ .  $P_i$  is some  $P_{s_i, s_j}$  calculated in step (3) and  $W_i$  is the  $W_{s_i, s_j}$  value of the dependent variable evaluated at the specified location from step (4) above.

### First moment

$$\mu_w = E[W] = \sum_{i=1}^{2^n} P_i W_i \quad (46)$$

## Second moment

$$\sigma_w^2 = E[(W - \mu_w)^2] = \sum_{i=1}^{2^n} P_i(W_i - \mu_w)^2 = \sum_{i=1}^{2^n} P_i(W_i)^2 - \mu_w^2 \quad (47)$$

## Third moment

$$\nu_w = \frac{E[(W - \mu_w)^3]}{\sigma_w^3} = \frac{1}{\sigma_w^3} \sum_{i=1}^{2^n} P_i(W_i - \mu_w)^3 = \frac{1}{\sigma_w^3} \sum_{i=1}^{2^n} P_i(W_i)^3 - 3\mu_w P_i(W_i)^2 + 2\mu_w^3 \quad (48)$$

### PEM Example: Unconfined triaxial compression of a $c'$ , $\phi'$ soil ( $n = 2$ )

This is the same example considered using the FOSM method earlier in the paper, involving drained unconfined triaxial compression of a  $c'$ ,  $\phi'$  soil. In the following sample calculation,  $\mu_{c'} = 100$  kPa and  $\mu_{\tan \phi'} = \tan 30^\circ = 0.577$ , and  $C.O.V._{c'} = C.O.V._{\tan \phi'} = 0.5$ .

Following the steps for implementing PEM:

1. The function to be evaluated is the same as equation (25), namely:

$$q_u = 2c' [\tan \phi' + (1 + \tan^2 \phi')^{1/2}] \quad (49)$$

2. It is assumed that the random shear strength variables  $c'$  and  $\tan \phi'$  are uncorrelated and lognormally distributed, thus from equations (38) and (39),

$$\begin{aligned} \xi_{c'_+} &= \xi_{\tan \phi'_+} = 2.10 \\ \xi_{c'_-} &= \xi_{\tan \phi'_-} = 0.48 \end{aligned} \quad (50)$$

3. The weights are determined for the four sampling points from equation (44) using equations (41) and (42) as follows:

$$\begin{aligned} P_{c'_+} &= P_{\tan \phi'_+} = 0.185 \\ P_{c'_-} &= P_{\tan \phi'_-} = 0.815 \end{aligned} \quad (51)$$

Therefore, from equation (44) with  $\rho_{ij} = 0$ , the sampling point weights are:

$$\begin{aligned} P_{++} &= 0.034 \\ P_{+-} &= P_{-+} = 0.151 \\ P_{--} &= 0.665 \end{aligned} \quad (52)$$

4. The dependent variable  $q_u$  is evaluated at each of the points. Table 4 summarises the values of the weights, the sampling points and  $q_u$  for this case:

**Table 4. Weights, sampling points and  $q_u$  values for PEM**

$P_{\pm\pm}$	$c'$	$\tan \phi'$	$q_{u\pm\pm}$
	(kPa)		(kPa)
0.034	205.0	1.184	1121.0
0.151	205.0	0.440	628.5
0.151	76.2	1.184	416.6
0.665	76.2	0.440	233.5

5. The first three moments of  $q_u$  can now be evaluated from equations (46), (47) and (48) as follows:

$$\mu_{q_u} = 0.034(1121.0) + 0.151(628.5) + 0.151(416.6) + 0.665(233.5) = 350.9 \text{ kPa} \quad (53)$$

$$\begin{aligned} \sigma_{q_u}^2 &= 0.034(1121.0 - \mu_{q_u})^2 + 0.151(628.5 - \mu_{q_u})^2 \\ &+ 0.151(416.6 - \mu_{q_u})^2 + 0.665(233.5 - \mu_{q_u})^2 = 41657.0 \text{ (kPa)}^2 \end{aligned} \quad (54)$$

$$\begin{aligned} \nu_{q_u} &= \frac{1}{\sigma_{q_u}^3} (0.034(1121.0 - \mu_{q_u})^3 + 0.151(628.5 - \mu_{q_u})^3 \\ &+ 0.151(416.6 - \mu_{q_u})^3 + 0.665(233.5 - \mu_{q_u})^3) = 2.092 \end{aligned} \quad (55)$$

Rosenblueth (1981) notes that for the multiple random variable case, skewness can only be reliably calculated if the variables are independent.

A summary of results for different  $C.O.V._{c', \tan \phi'}$  is presented in Table 5.

**Table 5. Statistics of  $q_u$  predicted using PEM**

$C.O.V._{c', \tan \phi'}$	$\nu_{q_u}$	$\sigma_{q_u}$	$\mu_{q_u}$	$C.O.V._{q_u}$
		(kPa)	(kPa)	
0.1	0.351	38.8	346.6	0.11
0.3	1.115	118.5	348.2	0.34
0.5	2.092	204.1	350.9	0.58
0.7	3.530	298.8	353.6	0.85
0.9	5.868	405.0	355.5	1.14

It is clear from a comparison of Tables 1 and 5 that FOSM and PEM give essentially the same results for this example problem.

## 5 Random Field/Finite Element Approach

For reasonably “linear” problems, the FOSM and PEM methods described in this paper are able to take account of soil property variability in a systematic way. The traditional methods however, typically take no account of spatial correlation, which is the tendency

for properties of soil elements “close together” to be correlated, while soil elements “far apart” are uncorrelated.

To address the correlation issue, the triaxial compression problem has been reanalysed using a random field/finite element approach (Random Finite Element Method or RFEM), that enables soil property variability and spatial correlation to be accounted for. The methodology involves the generation and mapping of a random field of  $c'$  and  $\tan \phi'$  properties onto a quite refined finite element mesh. Full account is taken of local averaging and variance reduction (Fenton and Vanmarcke 1990) over each element, and an exponentially decaying spatial correlation function is incorporated. An elasto-plastic finite element analysis is then performed using a Mohr-Coulomb failure criterion. Details of a similar analysis can be found in Griffiths and Fenton (2001). The mesh is then loaded axially until a maximum failure stress,  $q_u$  is reached. This failure load is recorded and the analysis is repeated numerous times using Monte-Carlo simulations. Each realisation of the Monte-Carlo process involves the same mean, standard deviation and spatial correlation length of soil properties. However the spatial distribution of properties varies from one realisation to the next so that each simulation leads to a different value of  $q_u$ . Following a “sufficient” number of realisations, the statistics (mean and standard deviation) of the output quantity  $q_u$  can then be computed. The analysis has the option of including cross correlation between properties and anisotropic spatial correlation lengths (e.g. the spatial correlation length in a naturally occurring stratum of soil is often higher in the horizontal direction). Neither of these options has been investigated in the current study to facilitate comparisons with the simpler forms of FOSM and PEM.

Lognormal distributions of  $c'$  and  $\tan \phi'$  have been used in the current study and mapped onto a square mesh of 400 8-node, quadrilateral, plane strain elements. The soil properties  $c'$  and  $\tan \phi'$  were assumed to be uncorrelated to each other ( $\rho = 0$ ). Typical realisations of the property distributions are shown in Figure 3 in the form of a grey scale in which weaker regions are darker, and stronger regions are lighter.

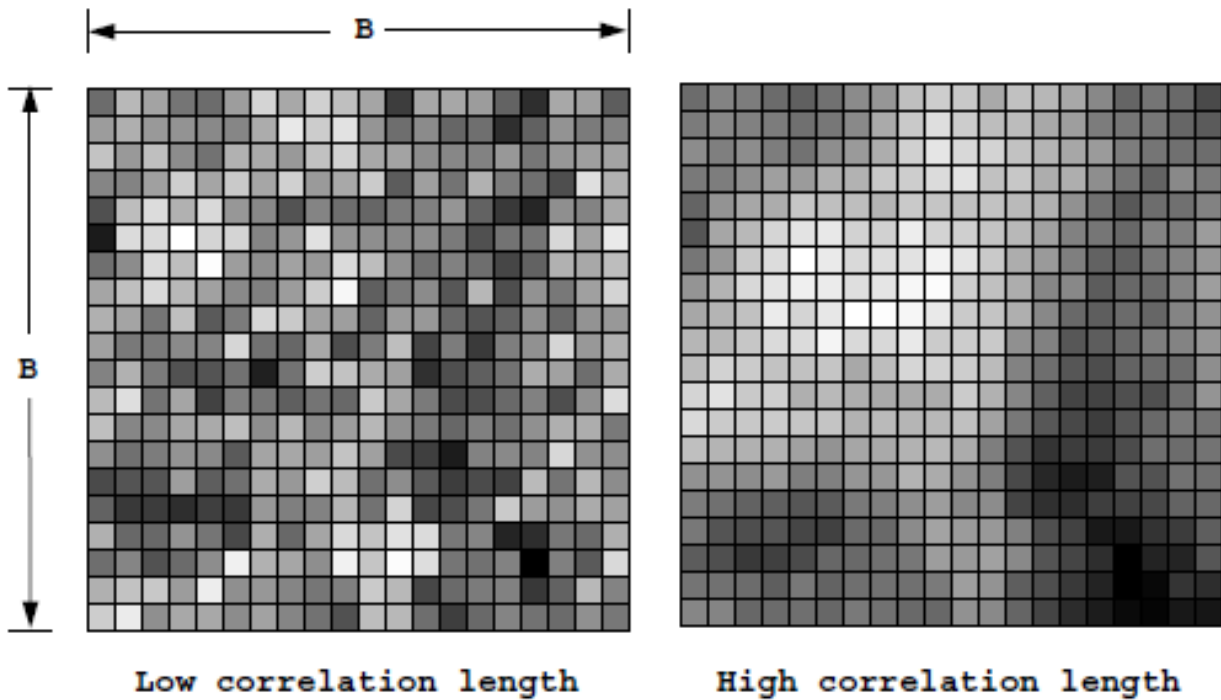


Figure 3: Typical random fields in the RFEM approach

An example of a relatively low spatial correlation length and a relatively high correlation length are shown. It should be emphasised that the mean and standard deviation of the random variable being portrayed are the same in both figures. The spatial correlation length (which has units of length) is defined with respect to the underlying normal distribution, and denoted as  $\theta_{\ln c', \ln \tan \phi'}$ . Both  $c'$  and  $\tan \phi'$  were assigned the same isotropic correlation length in this study. A convenient non-dimensionalisation of the spatial correlation length can be achieved in this case, by dividing by the side length  $B$  of the square mesh shown in Figure 3, thus  $\Theta = \theta_{\ln c', \ln \tan \phi'} / B$ .

### Parametric studies

In the resulting randomised finite element method (RFEM) studies, a series of analyses have been performed in which the coefficient of variations of  $c'$  and  $\tan \phi'$ , and spatial correlation length  $\Theta$  have been varied. In all cases, the mean strength parameters have been held constant at the same values considered earlier in the paper, namely  $\mu_{c'} = 100$  kPa and  $\mu_{\tan \phi'} = \tan 30^\circ = 0.577$ . The variation in the mean compressive strength,  $\mu_{q_u}$ , normalised with respect to the deterministic value based on the mean values  $q_u(\mu_{c'}, \mu_{\tan \phi'}) = 346.4$  kPa is shown in Figures 4a and 4b and the relationship between the coefficients of variation of input shear strength parameters and output compressive strength is shown in Figure 5. The following observations can be made from a comparison of the “simple” methods and the RFEM results.

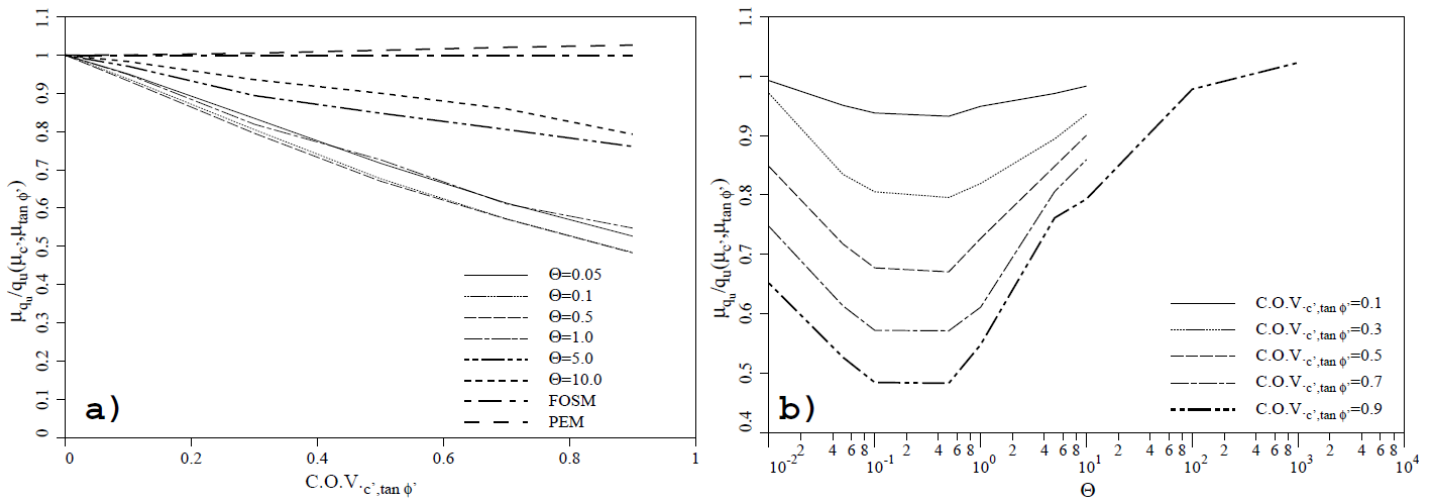


Figure 4: Variation of  $\mu_{q_u}$  with  $C.O.V._{c', \tan \phi'}$  and  $\Theta$

1) Figures 4a and 4b indicate that for intermediate values of  $\Theta$ , the RFEM results show a significant fall in  $\mu_{q_u}$  as  $C.O.V._{c', \tan \phi'}$  is increased. This is a very important difference from the FOSM and PEM methods, which both gave essentially constant  $\mu_{q_u}$ . In fact, the PEM and second order FOSM displayed a slight *increase* in  $\mu_{q_u}$ .

2) Figures 4b and 5 show that for large values of  $\Theta$ , the RFEM results tend to the FOSM/PEM predictions for all values of  $C.O.V._{c', \tan \phi'}$ , implying that the FOSM and PEM methods are special cases of RFEM with an infinite correlation length.

3) Figure 4b shows that the mean values of the compressive strength for all  $C.O.V._{c', \tan \phi'}$  display minima at around  $\Theta = 0.2$ .

4) At very small  $\Theta$ , an increase in  $\mu_{q_u}$  is observed as it heads back towards the compressive strength based on the median shear strength values. These theoretical results have been included in Figure 4b. As a sample calculation, the result corresponding to  $C.O.V._{c', \tan \phi'} = 0.5$  when  $\Theta \rightarrow 0$  are given by

$$Median_{c'} = \mu_{c'} / (1 + C.O.V._{c', \tan \phi'}^2)^{1/2} = 89.44 kPa$$

$$Median_{\tan \phi'} = \mu_{\tan \phi'} / (1 + C.O.V._{c', \tan \phi'}^2)^{1/2} = 0.5146$$

thus

$$\mu_{q_u} / q_u(\mu_{c'}, \mu_{\tan \phi'}) \rightarrow 0.8479$$

5) Figure 5 indicates that the FOSM and PEM methods, without accounting for spatial correlation, give  $C.O.V._{q_u} \approx C.O.V._{c', \tan \phi'}$  implying that the variability of the compressive strength  $q_u$  is essentially the same as the variability of the input parameters  $c'$  and  $\tan \phi'$ . The RFEM results however, including the effects of spatial correlation, indicate a steady reduction in the  $C.O.V._{q_u}$  as  $\Theta$  is decreased.

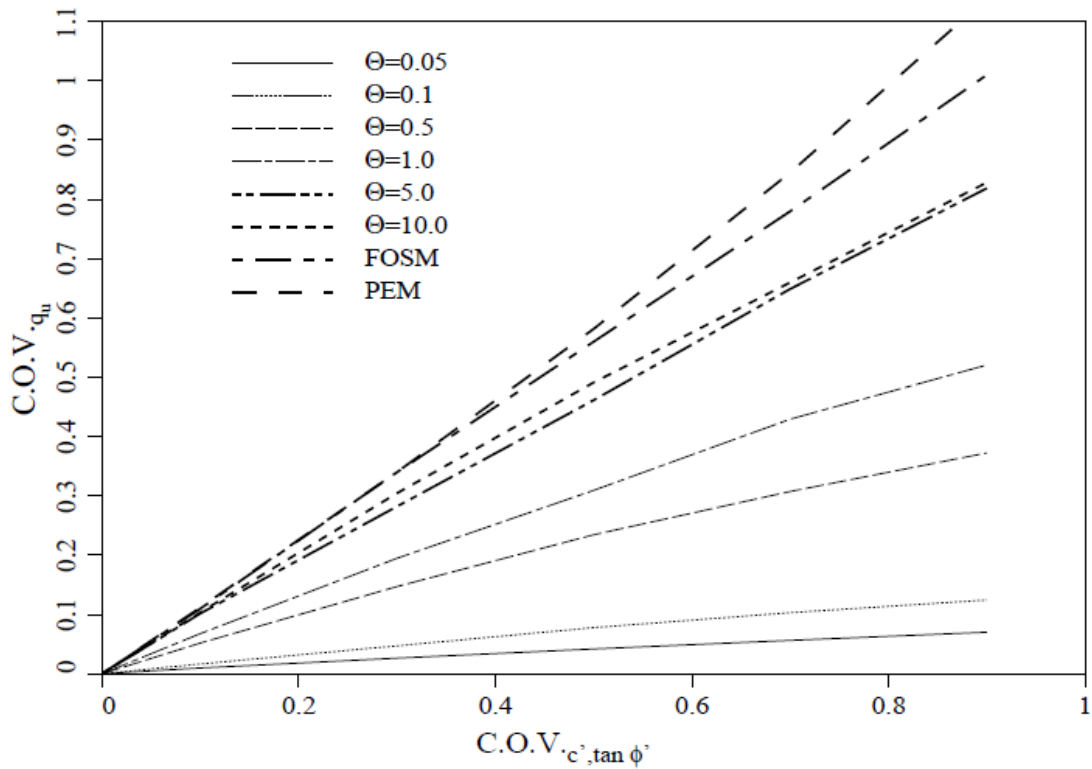


Figure 5:  $C.O.V._{q_u}$  vs.  $C.O.V._{c', \tan \phi'}$



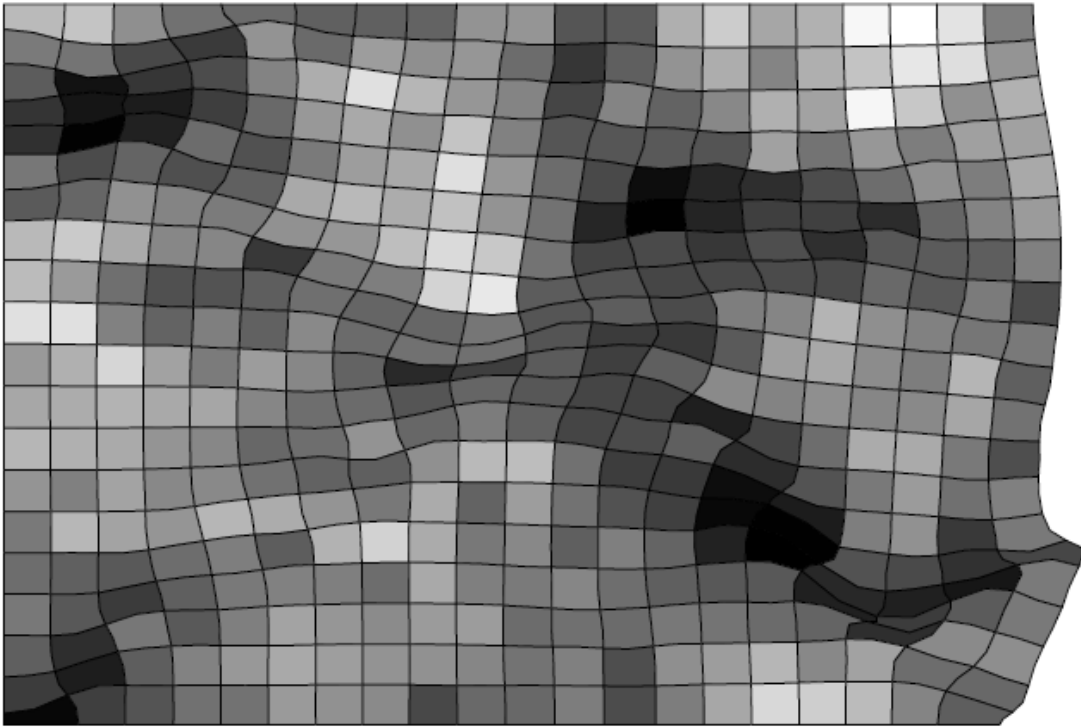


Figure 6: Typical deformed mesh at failure

6) Figure 6 shows a typical mesh at failure from the RFEM analysis. It illustrates the meandering and irregular nature of the failure surface which is attracted to the dark (weaker) zones.

## 6 Discussion and concluding remarks

The paper has demonstrated three methods for implementing probabilistic concepts into geotechnical analysis of a simple problem of compressive strength. The “simple” methods were the First Order Second Moment (FOSM) and Point Estimate Method (PEM), and the “sophisticated” method was a Random Finite Element Method (RFEM) method. The output statistics of the compressive strength by FOSM and PEM were similar to each other, but differed significantly from the RFEM method.

1) Probabilistic methods offer a more rational way of approaching geotechnical analysis, in which probabilities of design failure can be assessed. This is more meaningful than the abstract “Factor of Safety” approach. Being relatively new however, probabilistic concepts are difficult to digest, even in the so called “simple” methods.

2) The RFEM method actually models the physical locations of weak and strong zones within the specimen. When the soil block is compressed, progressive failure occurs, and the failure mechanism “seeks-out” the weakest path through the soil. Figure 6 clearly shows how the failure mechanism is attracted to the weaker (darker) regions of the mesh. The traditionally applied FOSM and PEM have no concept of local zones of weakness that can dominate the compressive strength.

3) The RFEM method indicates a significant reduction in mean compressive strength due to the weaker zones dominating the overall strength at intermediate values of  $\Theta$ . The observed reduction in the mean strength by RFEM, is greater than could be explained by local averaging alone. As the value of  $\Theta$  is reduced further, however, there is a gradual increase in the value of  $\mu_{qu}$  as shown in Figure 4b. From a theoretical point of view, as  $\Theta$  becomes vanishingly small,  $\mu_{qu}$  will continue to increase towards a deterministic value based on the *median* of the input shear strength parameters. As the spatial correlation length decreases, the weakest path becomes increasingly tortuous and its length correspondingly longer. As a result, the weakest path starts to look for shorter routes cutting through higher strength material. In the limit, as  $\Theta \rightarrow 0$ , the optimum failure path is expected to be the same as in a uniform material with strength equal to the median. A very fine mesh would be needed to show this effect numerically.

4) The paper has shown that proper inclusion of spatial correlation, as used in the RFEM, is essential for quantitative predictions in probabilistic geotechnical analysis. While “simpler” methods such as traditional FOSM and PEM are useful for giving guidance on the sensitivity of design outcomes to variations of input parameters, their inability to systematically include spatial correlation and local averaging severely limits their usefulness.

5) The paper has shown that the RFEM is the only currently available method able to properly account for the important influence of spatial correlation and local averaging in stability problems involving highly variable soils. It is anticipated that probabilistic approaches to geotechnical analysis will increase in popularity, however it may take time before the methods become acceptable in routine geotechnical investigations.

## References

- [1] J.R. Benjamin and C.A. Cornell. *Probability, statistics and decision making for civil engineers*. McGraw Hill, London, New York, 1970.
- [2] J.T. Christian and G.B. Baecher. Point-estimate method as numerical quadrature. *J Geotech Geoenviron Eng, ASCE*, 125(9):779–786, 1999.
- [3] G.A. Fenton and E.H. Vanmarcke. Simulation of random fields via local average subdivision. *J Eng Mech, ASCE*, 116(8):1733–1749, 1990.
- [4] D.V. Griffiths and G.A. Fenton. Bearing capacity of spatially random soil: the undrained clay Prandtl problem revisited. *Géotechnique*, 51(4):351–359, 2001.
- [5] M.E. Harr. *Reliability based design in civil engineering*. McGraw Hill, London, New York, 1987.
- [6] E. Rosenblueth. Point estimates for probability moments. In *Proc. Nat. Acad. Sci. USA*, number 10, pages 3812–3814. 1975.
- [7] E. Rosenblueth. Two-point estimates in probabilities. *Appl. Math. Modelling*, 5:329–335, 1981.

**Acknowledgement**

The writers acknowledge the support of NSF Grant No. CMS-9877189.